

2023

Development of Drug-Drug Interaction Research Techniques Involving the CYP3A4 Human Liver Enzyme

Sarah Iacoviello

Follow this and additional works at: <https://digitalcommons.assumption.edu/honorstheses>

 Part of the [Life Sciences Commons](#)

DEVELOPMENT OF DRUG-DRUG INTERACTION RESEARCH TECHNIQUES
INVOLVING THE CYP3A4 HUMAN LIVER ENZYME

Sarah Iacoviello

Faculty Supervisor: Dr. Edward Dix

Department of Biological and Physical Sciences

A Thesis Submitted to Fulfill the Requirements of the
Honors Program at Assumption University

Spring 2023

*JMJ***Table of Contents**

Abstract.....	3
Introduction.....	4
Drug Development Process.....	4
Liver Microsomes and Drug Metabolism.....	6
The Cytochrome P450 Enzymes.....	7
Cytochrome P450 Mechanism.....	8
Drug-Drug Interactions.....	9
Goals and Description of Our Project	11
Methods, Results, and Discussion.....	12
Trans-Stilbene Oxide Synthesis.....	12
Method.....	12
Results.....	13
Discussion.....	16
Carbamazepine-10,11-epoxide Synthesis.....	17
Method.....	17
Results.....	18
Discussion.....	23
HPLC Calibration Curves for Carbamazepine and Carbamazepine-10,11-epoxide.....	24
Method.....	24

Results.....	25
Discussion.....	29
Sample Calculation.....	30
Solution and Microsome Preparation.....	31
Microsomal Metabolism of CBZ.....	32
First Metabolism of CBZ.....	32
Method.....	32
Results.....	34
Discussion.....	35
Second Metabolism of CBZ with Controls.....	35
Method.....	35
Results.....	36
Discussion.....	38
Conclusion.....	39
References.....	41

Abstract

Understanding the metabolic pathway of a drug is an integral part of pharmaceutical development. Microsomal metabolism is the industry standard to model the metabolism of the drug by the liver *in vitro*. Our studies employ carbamazepine (CBZ) as a CYP3A4 substrate to develop a method to investigate potential drug-drug interactions involving this enzyme. Toward this end, the metabolite of CBZ, carbamazepine-10,11-epoxide (CBZ-E), was synthesized for use as a standard. The purity of the synthesized CBZ-E was 95.2%, and the percent yield was 76.16%. The use of human liver microsomes is a common incubation method used to model drug metabolism in an *in vitro* setting. At this time, we have begun to develop techniques for analyzing the human metabolism of CBZ with a view toward using this pathway to probe drug-drug interactions. However, we have yet to perform a completely successful metabolism of CBZ. Potential problems with our method may be in the HPLC analysis or in the low concentration of microsomal protein. Efforts on this project continue.

Introduction

~ Drug Development Process ~

Obtaining approval from the Food and Drug Administration (FDA) for the use and sale of a drug is a lengthy and involved process. The average time it takes a pharmaceutical company to develop one drug out of the thousands of failed compounds is at least 10 years with a cost of about \$2.6 billion.¹ During these 10 years of development there are two main stages: the discovery process, and the clinical trials. The discovery process takes approximately 3 to 6 years. It begins with pre-discovery when a condition or disease is identified and understood. The biological molecules, which produce the desired clinical effect when manipulated by a drug, are then identified. These are known as the biological target molecules. From here, the process transitions to the proper drug discovery portion of the first stage. Thousands of candidate compounds are tested with the biological target molecules. These tests rule out any ineffective drugs, and they indicate potential lead compounds so that only a few of the thousands of compounds will continue in the process. The lead compounds then undergo the early safety testing. Predictions regarding how the drug behaves in the human body are made in this stage. These predictions include how the drug is *absorbed*, its *distribution*, the *metabolites* it forms, *excretion* from the body, and any potential risks concerning *toxicity* of metabolites or any other aspect of its pathway (ADMET). The lead compounds are then put through the process of optimization in which the structure of the compound is varied to optimize its effectiveness and minimize the resulting side effects. Hundreds of variations are tested and narrowed down to a few candidate drugs. These lead compounds then undergo preclinical testing where they are put through both *in vitro* and *in vivo* testing using animal models. In this stage, the mechanism of

the drug's action and any potential side effects are determined. These steps complete the discovery process of the drug.¹

Before clinical trials can begin, an investigational new drug (IND) application must be submitted to the FDA. This application must include all the preclinical results, a detailed prediction of how the drug will work in the human body, any potential side effects, information on manufacturing the drug, and a plan for the clinical trial including how it will be performed, where it will take place, and who will carry it out. In addition to the FDA's approval, the institutional review board (IRB) or the ethical committee (EC) of the institution where the trial will take place must approve the trial and monitor it through the process. The IRB/EC has the right to terminate or accelerate the trial at any time.¹

Once the drug has received approval from the FDA and the location specific IRB/EC, the clinical trials begin. On average, these trials take 6-7 years to complete and they have a less than 12% success rate. There are three phases in the clinical trials. In phase I, the drug is tested on less than 100 healthy volunteers. These tests are to assess the safety/toxicity of the drug, its absorption, metabolism, elimination from the body, and any side effects. This stage also helps to determine safe dosage of the drug. In phase II, 100-500 patients with the condition to be tested volunteer. These trials are compared with a placebo drug or the accepted treatment of the condition. In this stage, the dosage (mg/kg) and the schedule for the administration of the drug are determined. Phase III includes more than 1,000 patients across the world. In this phase, the drug's safety and efficacy are tested along with its interaction with other medicines. Out of all three phases, phase three is the most complex because it involves coordination and data analysis across hundreds of sites. The FDA and the local IRB/EC must constantly be monitoring the

trials. In addition, the company is responsible for manufacturing enough quality products for all the trials, and the final FDA approval application is also begun during this phase.¹

Once the clinical trials are complete a new drug application (NDA) or a biologics license application (BLA) is submitted to the FDA. These consist of the results and data analysis from the entire process from the development to the clinical trials. These applications are usually more than 100,000-page documents. After the FDA has approved the application, the drug is manufactured on a large scale and the company continues to monitor it.¹

~ *Liver Microsomes and Drug Metabolism* ~

Liver microsomes are not natural formations in the cell. Rather, they form when the liver cells are homogenized, and the newly formed microsomes are separated from the rest of the cell through fractional centrifugation.² Essentially, the endoplasmic reticulum is broken up in the process of homogenization and forms vesicles. Because the endoplasmic reticulum, specifically in the liver cells, makes and contains enzymes which metabolize drugs, the vesicles which form from the homogenization of this organelle contain the drug-metabolizing enzymes.³ As a result, the isolated microsomes can be used to test the effects of these enzymes in drug metabolism and the resulting metabolites without the complication of working with the entire cell.

The main outcome of drug metabolism is a chemical change in the drug compound to make it a more polar molecule so that it will dissolve in water and be carried out of the body. There are two “phases” in drug metabolism. Phase I metabolism involves the dealkylation of an electronegative atom, or hydroxylation. Phase II involves conjugation of the substrate with a more polar molecule.⁴ Both of these pathways produce a more soluble metabolite that will be carried out of the body. For our purposes only phase I metabolism will be considered.

~ *The Cytochrome P450 Enzymes* ~

The main enzymes involved in drug metabolism by the liver are the cytochrome P450 (CYP) enzymes which are responsible for the phase I metabolism. The CYP enzyme is fairly consistent in its structure and general function (that of polarizing drugs) among species including humans. However, the structure of the CYP enzymes vary resulting in different substrate specificity.⁵ All CYP enzymes belong to the P450 superfamily which is then divided into a family indicated by a number after the 'CYP' abbreviation (e.g. CYP1). The enzymes in the families are at least 40% identical to each other in structure. A capital letter follows the number which indicates to which subfamily the enzyme belongs (e.g. CYP1A). In a given subfamily the structure of the enzymes should at a minimum be 55% identical. Following the letter, which indicates the subfamily of the enzyme, comes a second number indicating an individual enzyme (e.g. CYP1A2). For two enzymes to be categorized as different from one another (being given a different final number in their name), they must differ by at least 3% or more in structure.⁶ As a result, because all the CYP enzymes are identical over a large portion of their structures, they all metabolize drugs using roughly the same general mechanism. That is they all work to polarize the molecule so that it becomes soluble and is flushed out of the body. The differences in the structure between families and subfamilies result in the enzyme metabolizing different drugs, or the enzymes will metabolize the same drug but the process will, in many cases, result in different metabolites. All mammals contain CYP enzymes; however, all mammals do not contain the same combination or concentration of the different types of CYP enzymes. These differences result in variations in drug metabolism across species.⁷

~ Cytochrome P450 Mechanism ~

The cytochrome P450 enzymes are able to destabilize relatively stable bonds in order to react with the molecule and turn the drug into a more polar form. They do this by utilizing redox and radical chemistry in their iron-containing porphyrin ring (Figure 1).

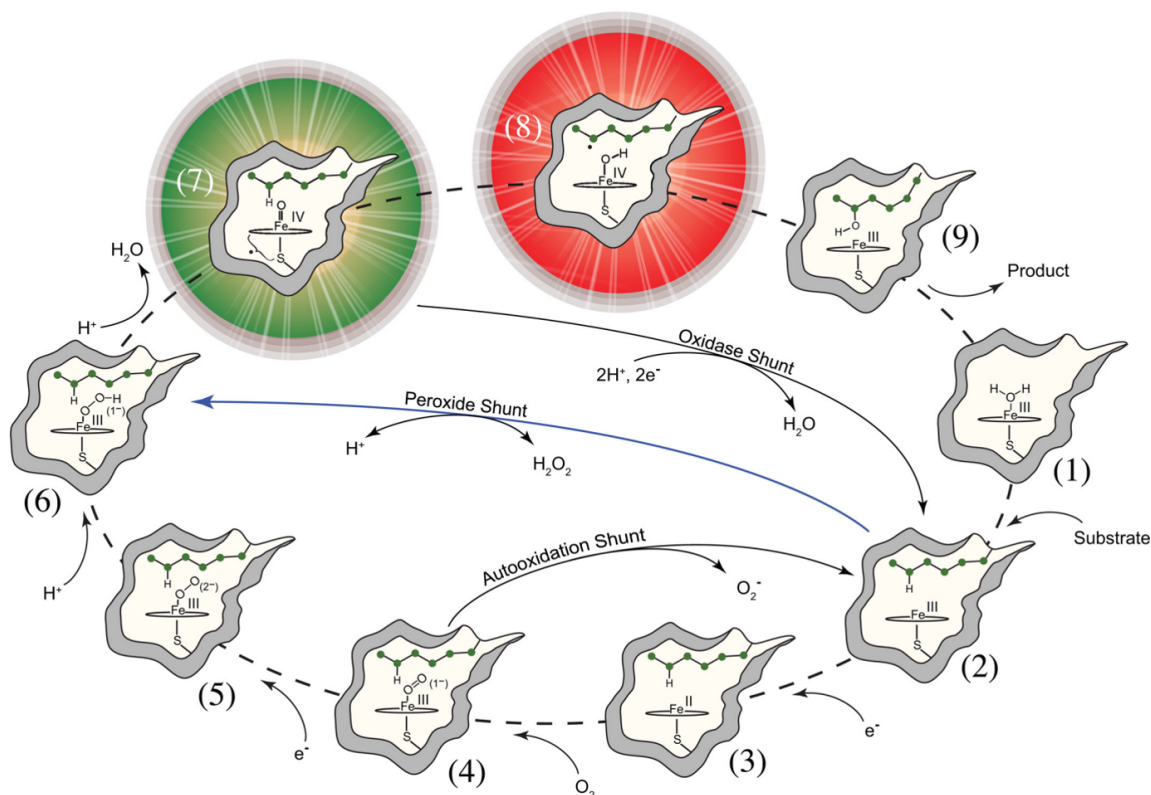


Figure 1. Mechanism of a cytochrome P450 enzyme presented by Krest *et al.*⁸

In this representative example of the metabolism mechanism, the first step of the mechanism involves the binding of the substrate to a location other than the iron containing porphyrin ring of the protein, while the protein is in low spin. Through the dissociation of water in a different location of the enzyme, prompted by the binding of the substrate, an electron is transferred to the iron, changing it from Fe(III) to Fe(II), from low to high spin. An oxygen

molecule then binds to the iron, the iron donates an electron to the O_2 so that the distal oxygen takes on a charge of -1. The double bond between the two oxygens is then donated to the distal oxygen, causing it to take on a charge of -2 forming a ferric peroxo complex. The distal oxygen is then protonated forming a ferric hydroperoxo complex. A second proton breaks the bond between the two oxygens so that a water molecule is produced and the remaining oxygen forms a double bond and a radical with the iron, changing it from Fe(III) to Fe(IV). The radical formed in this process is higher in energy than a carbon radical, and as a result, the iron-oxygen radical complex pulls a hydrogen off the substrate forming a carbon radical on the substrate. The carbon radical then pulls the hydroxyl group from the iron, reducing Fe(IV) to Fe(III), and completing the radical. The substrate is then released having been made more polar due to the addition of the hydroxyl group, and the enzyme is left in its original state, ready to act again.⁸ While this is the mechanism for hydroxylation, the mechanism for epoxidation, while not as well known, likely follows a similar path.

~ *Drug-Drug Interactions* ~

A drug-drug interaction occurs when two drugs are metabolized by the same enzyme. Rather than having the enzyme work on one drug, it is forced to work on two or multiple drugs. As a result, the rate of metabolism of one or both of the drugs is significantly decreased because the enzyme is “preoccupied.” With this decrease in the rate of metabolism, the blood concentration of the drug in the body increases because it is not being removed from the body fast enough. With this increase of drug concentration, the levels of toxicity and potentially the fatal level of toxicity for the drug may be reached.⁹

While the CYP enzymes are the main phase I metabolizing enzymes, each family and, more specifically, subfamily of CYP enzymes do not act on every drug. They each have their own set of drugs or substrates upon which they can act. The most common drug metabolizing enzyme in humans is the CYP3A4 enzyme. The CYP3A4 enzyme makes up 30% of the total protein in the liver, and it metabolizes about 50% of the metabolically eliminated drugs on the market. As a result, the risk for drug-drug interactions involving the CYP3A4 enzyme is very high.⁹

These interactions do not only occur between two drugs. Rather they may also occur between a drug and a food or herb. Because of the CYP3A4 enzyme's ability to metabolize a wide variety of substrates, interactions involving any of these substrates are very common. For example, CYP3A4 metabolizes a compound in grapefruit, and as a result, if an individual consumes grapefruit while he is taking a drug metabolized by CYP3A4, he will experience a food-drug interaction and will be at risk of an overdose even though he took the prescribed dose of the drug.⁹ Not only is one at risk of a drug overdose during a drug-drug interaction, but the interaction may also offset the relative proportions of the enzymes in the body when it occurs. For example, if one of the two substrates in the interaction activates the xenobiotic nuclear receptor PXR or is an inducer, more of the enzyme responsible for the metabolism will be produced by the body. As a result, the body will metabolize the drugs involved with this enzyme at a different rate than expected which may lead to toxicity problems.⁹

Because of CYP3A4's versatility and the potential versatility of the other cytochrome enzymes, the FDA requires extensive research into the potential drug-drug interactions which may be induced by new or existing medications. As CYP3A4 is known for its versatility, the

drug-drug interactions involving this enzyme are well researched.⁹ As a result, metabolism by the 3A4 enzyme is a useful tool to act as a control in new or existing research methods.

~ **Goals and Description of Our Project** ~

The goal of our project was to develop a method by which drug-drug interactions could be investigated using the equipment available to Assumption University. The enzyme CYP3A4 was used because its metabolic parameters are well documented and could easily be compared with literature values. The substrate used was carbamazepine (CBZ) as it is mainly metabolized by CYP3A4.¹⁰ The main metabolite of CBZ, carbamazepine-10,11-epoxide¹⁰ (CBZ-E), was synthesized and identified. The parameters for the HPLC analysis to separate, identify, and quantify the two were then determined. Lastly, the metabolism of CBZ was run and the progress of the epoxide formation was monitored over time.

Methods, Results, and Discussion

~ *Trans-Stilbene Oxide Synthesis* ~

Before the synthesis of CBZ-E, the epoxidation method was tested on t-stilbene for its effectiveness as t-stilbene is a cheaper compound with a comparable structure to that of CBZ.

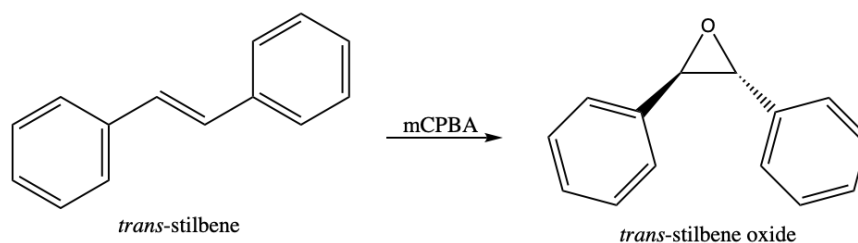


Figure 2. Reaction scheme

Method:

The procedure for the synthesis of styrene oxide¹¹ was modified for trans-stilbene. Trans-stilbene (0.541g, 3.00 mmol) was added to 5mL dichloromethane. While the solution was stirred over ice, 0.533g mCPBA (3.09 mmol) was added and a reflux column was fitted on the flask (water was not run through the reflux column as the presence of the column was a precaution to catch any potential fumes from the solvent or overflow from the reaction). The reaction was kept on ice for 4 hours and then left to come to room temperature. The progress of the reaction was monitored by dissolving a drop of the reaction in ethyl acetate and running it on a TLC (silica gel 60 F₂₅₄) plate with hexanes as the mobile phase and unreacted t-stilbene as a comparison standard. Three days into the reaction, 0.750g mCPBA (4.35 mmol) was added to push the reaction to completion.

When the TLC indicated that the reaction was complete, the solution was washed with 2mL 2.8M NaOH five times to extract both the reacted and unreacted mCPBA. The solution was then dried using calcium chloride and the solvent was drawn off with the rotovap. The product was analyzed using ^1H NMR and IR spectroscopy.

Results:

Upon the addition of mCPBA, the reaction precipitated a white solid, which dissolved easily in ethyl acetate. Table 1 contains the R_f values of t-stilbene, the product, and the mCPBA which were 0.61, 0.23, and 0.13 respectively. The TLC indicated that the reaction was complete after 5 days by the absence of t-stilbene. The mass of the product was 0.206 g (1.05 mmol) which was a 35.0% yield.

Table 1. R_f values for the TLC analysis

Compound	R_f value
t-stilbene	0.61
product	0.23
mCPBA	0.13

Figures 3 and 4 contain the NMR spectra for the t-stilbene and the synthesized product respectively. Table 2 contains the peak shifts present in the spectra. The product had the same peak shifts as the t-stilbene with an additional peak at 3.867ppm. However, the peaks around 7.25ppm were closer together in the product. All three spectra had the shifts found in the deuterated chloroform.

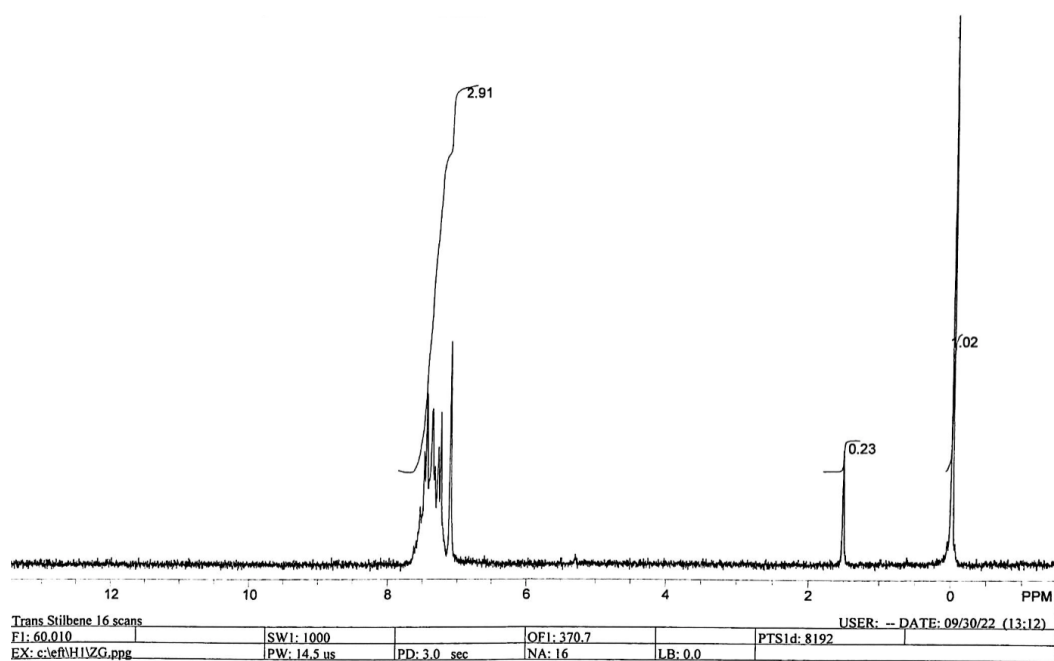


Figure 3. NMR spectrum of the t-stilbene.

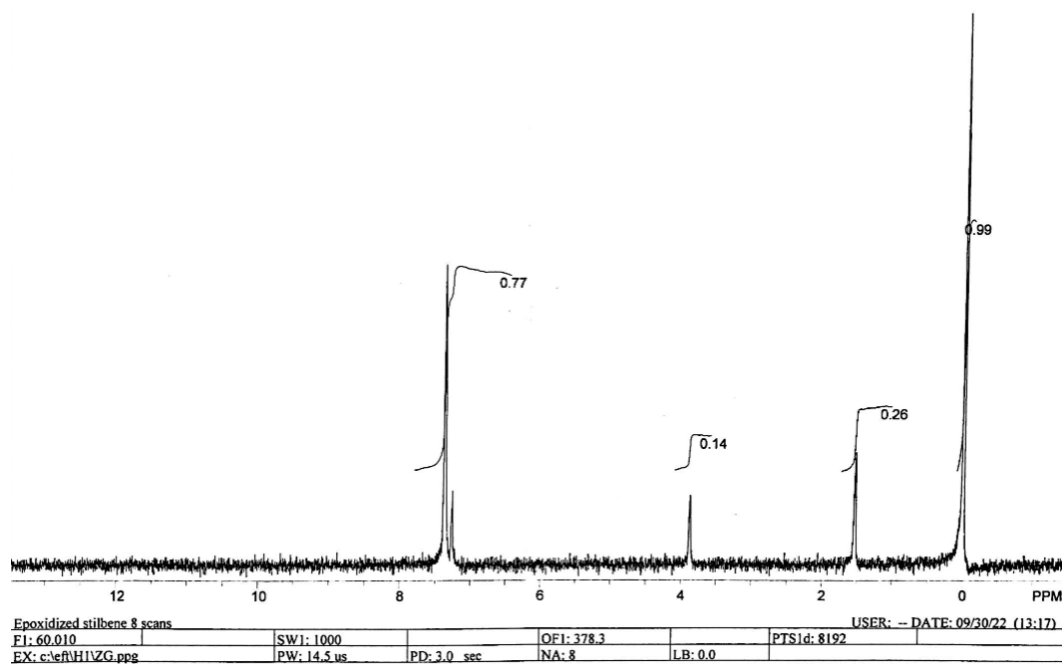


Figure 4. NMR spectrum of the product.

Table 2. Peak shifts in the NMR spectra.

Compound	Shift (ppm)	Corresponding proton
t-stilbene	1.518	H ₂ O
	7.110	Alkene
	7.251 - 7.454	Alkene (vinyl C-H)
Product	1.534	H ₂ O
	3.867	Benzylic C-H, epoxide C-H
	7.259	CHCl ₃
	7.361	Aromatic

Figure 5 contains the IR spectra for the deuterated chloroform, t-stilbene, and the product. The two signals at 1450 cm⁻¹, characteristic of the alkene bond linking the two aromatic rings in the t-stilbene, were absent in the spectrum of the product. In the product, there was no signal in the 3200 - 3600 cm⁻¹, the typical region for an OH bond.

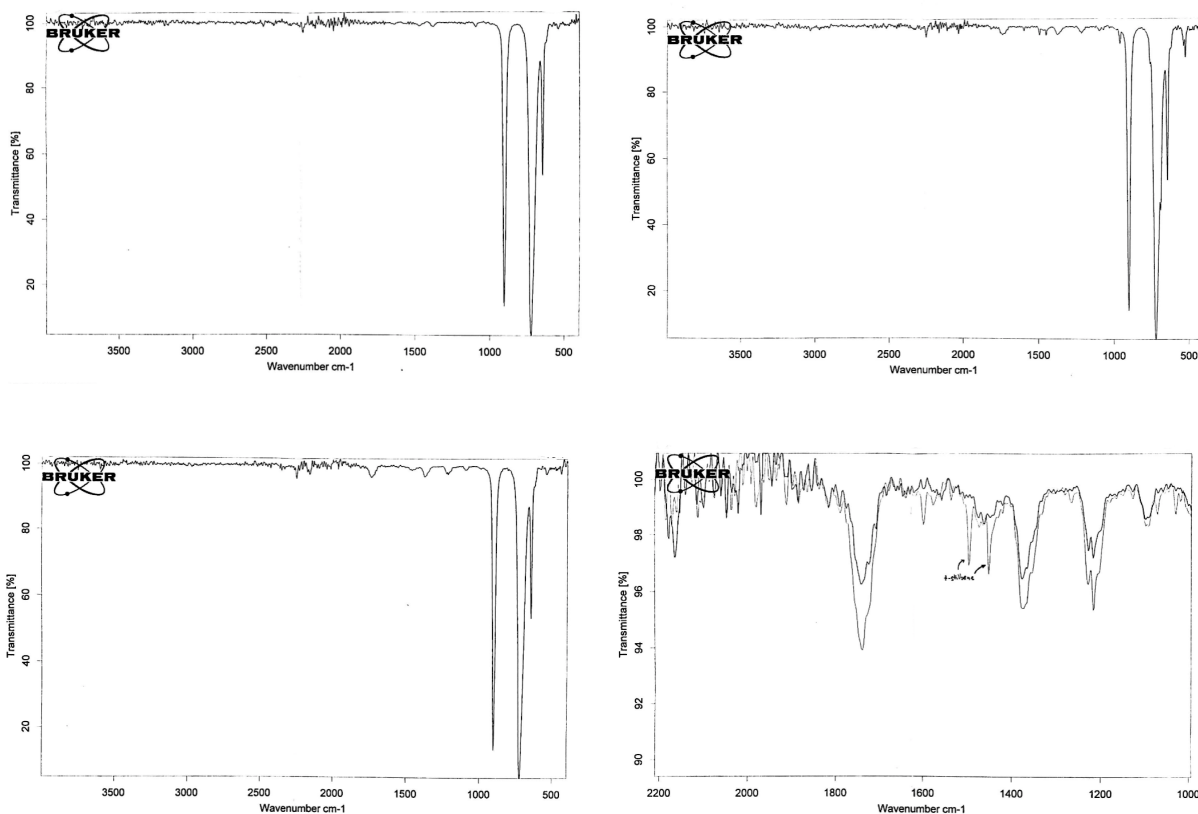


Figure 5. IR spectra for chloroform-D (top left), t-stilbene (top right), product (bottom left), and the product superimposed on t-stilbene (bottom right). The indicated peaks on the superimposed spectra are those of t-stilbene.

Discussion:

The product was *trans*-stilbene oxide. The IR spectra (Figure 5) did not indicate the appearance of a hydroxyl group in the product, which would have indicated hydrolysis of the epoxide, and the two peaks indicating the alkene linking the two aromatic rings disappeared in the product. The NMR spectra indicated the addition of an oxygen singly bonded to carbon and the disappearance of the alkene (Table 2). Therefore, because the oxygen was not in the form of a hydroxyl group and it was singly bonded, it formed an epoxide ring with two neighboring carbons resulting in *trans*-stilbene oxide.

~ Carbamazepine-10,11-epoxide Synthesis ~

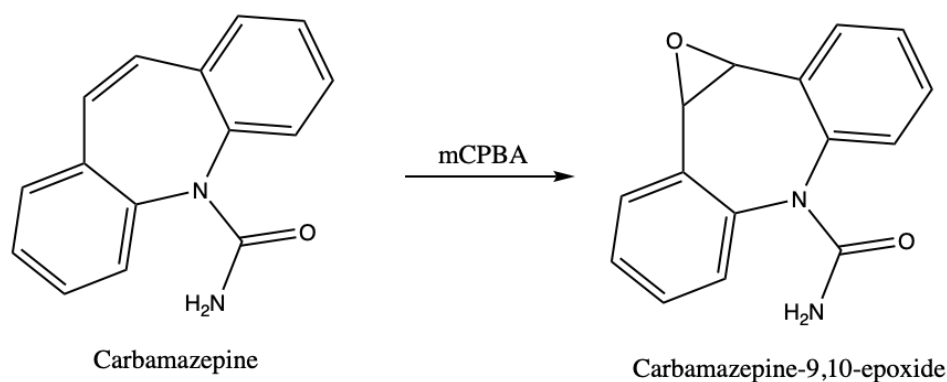


Figure 6. Epoxidation reaction scheme

Method:

The procedure for the synthesis of styrene oxide¹¹ was modified for the synthesis of carbamazepine-10,11-epoxide. Carbamazepine (CBZ) (0.094g, 0.398 mmol) was added to 5mL dichloromethane. While the solution was stirred over ice, 0.187g mCPBA (1.08 mmol) was added and a reflux column was fitted on the flask (water was not run through the reflux column). The reaction was left to come to room temperature. The progress of the reaction was monitored using TLC (silica gel 60 F₂₅₄) with 1:1 hexanes and acetone as the mobile phase and unreacted CBZ and mCPBA as comparison standards. Because the reaction was not proceeding to completion after one day, 0.101g mCPBA (0.585 mmol) was added to the reaction.

After three days, the solution was washed with 2mL 2.5M NaOH three times and then twice with H₂O to extract both the reacted and unreacted mCPBA. The reaction was then dried using calcium chloride and the solvent was drawn off with the rotovap. The product was analyzed using ¹H NMR spectroscopy, set to take 16 scans and with a gain of 45, and IR

spectroscopy, set to 8 scans. When the reaction mixture was not being worked on, it was refrigerated.

Results:

The reaction remained dissolved and clear for several days. It then took on a yellow color and began to form an orange precipitate at which point the reaction was quenched. The R_f values for the TLC are located in Table 3. The mCPBA traveled the farthest ($R_f = 0.8$), followed by the CBZ ($R_f = 0.52$), followed by the product ($R_f = 0.32$). In the presence of UV light, the product fluoresced (Figure 7). The mass of the product was 0.080g (0.317 mmol, if 100% pure) which was an 80% yield.

Table 3. R_f values for the TLC analysis

Compound	R_f value
mCPBA	0.8
Carbamazepine	0.52
Product	0.32

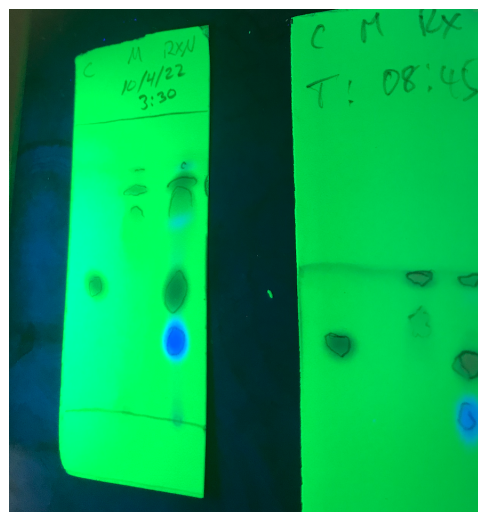


Figure 7. TLC of the reaction in progress.

When the reaction was quenched with the 2.5M NaOH, the reactants and product formed an oily green mass which slowly changed to a light yellow in color (Figure 8 left). When the water was added, the reaction mixture cleared up into a yellow solution (Figure 8 right).

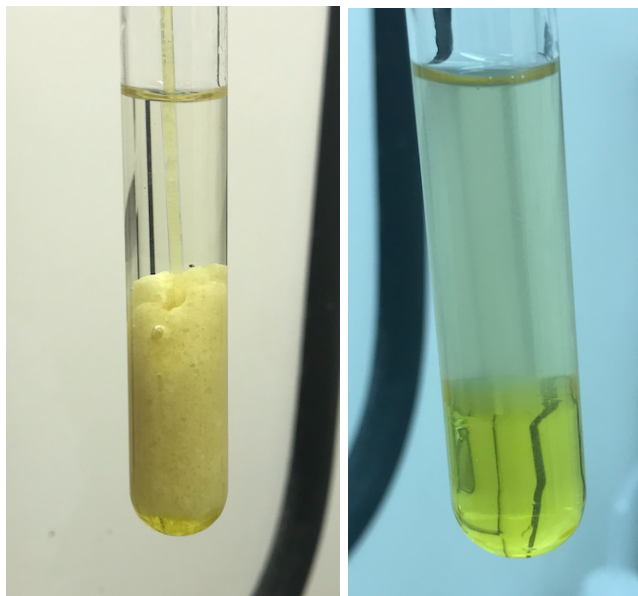


Figure 8. Emulsion formed during the NaOH wash (left), demulsification followed by the addition of H₂O (right).

Figures 9 and 10 contain the ¹H NMR spectra, and table 4 contains the peak shifts. In the spectrum for CBZ, there was a peak at 6.944 ppm indicating the alkene uninvolved in the aromatic rings. This peak was not present in the spectrum for the product, and there was a new peak at 4.272 ppm which was consistent with a shift of a proton on a carbon singly bonded to an oxygen. There was also an additional peak in the product at 1.644 ppm which was attributed to water.

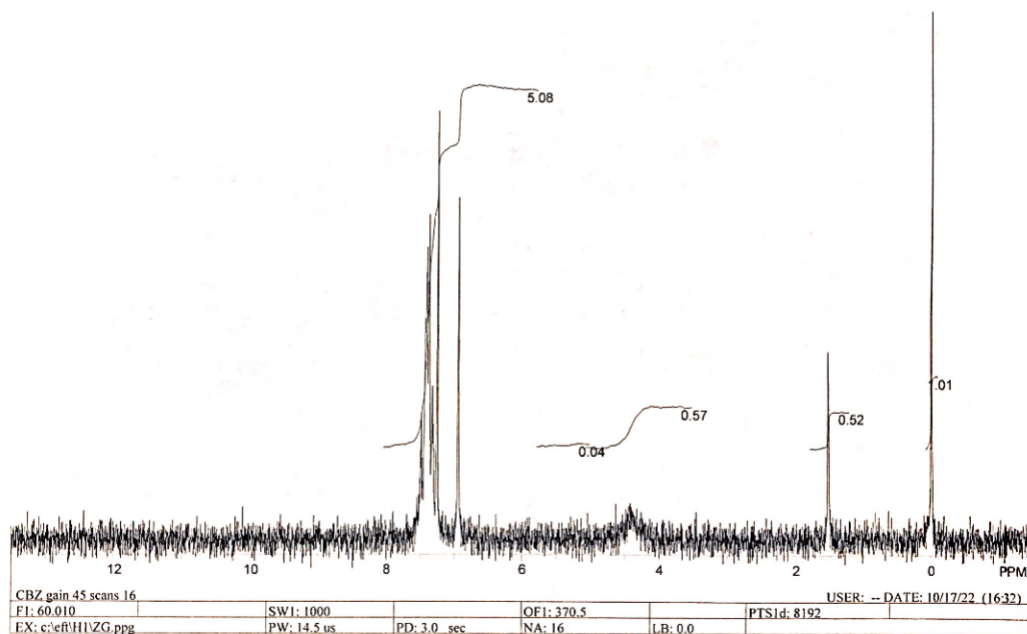


Figure 9. ^1H NMR spectrum for carbamazepine.

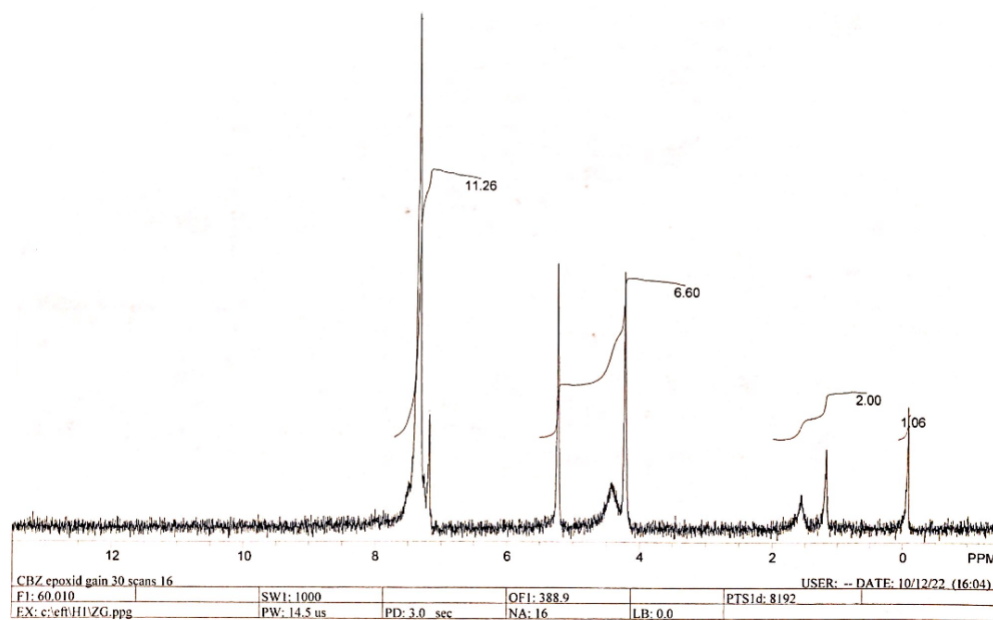


Figure 10. ^1H NMR spectrum for the product.

Table 4. ^1H NMR chemical shifts

Compound	Shift (ppm)	Corresponding proton
Carbamazepine	1.536	H ₂ O
	4.409	Carbamide
	6.944	Alkene
	7.257	CHCl ₃
	7.332 - 7.493	Aromatic Ring
Product	1.257	Impurity
	1.644	H ₂ O
	4.272	Epoxide Proton (Potential)
	4.492	Carbamide
	5.294	dichloromethane
	7.257	CHCl ₃
	7.411	Aromatic Ring

Figures 11 and 12 contain the IR spectra data for CBZ and the product. In both spectra, peaks are present at 1680, 1580, 1500, and 1400 cm^{-1} indicating the presence of alkenes in both compounds. The product spectra did not contain a peak in the 3200 to 3600 cm^{-1} range indicating that the potentially formed epoxide ring was not hydrolyzed.

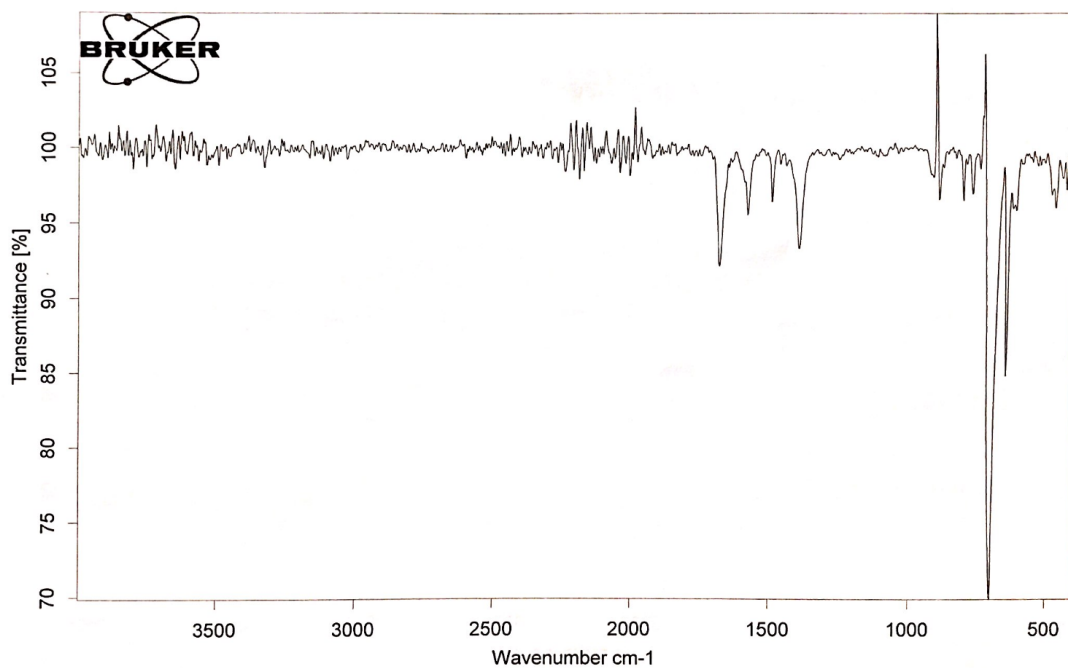


Figure 11. IR spectrum of the carbamazepine.

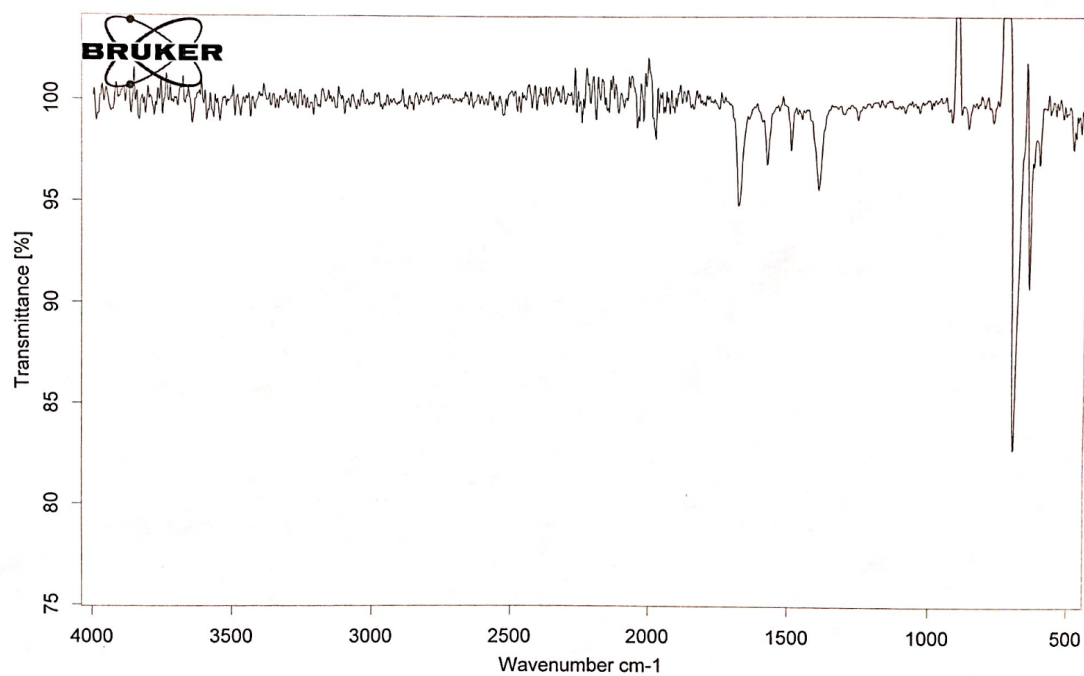


Figure 12. IR data for the product

Discussion:

The identity of the product as carbamazepine-10,11-epoxide was supported. Because the IR spectra did not indicate the presence of hydroxides (Figure 12), and the NMR spectra indicated the addition of a carbon oxygen single bond and the disappearance of the alkene on the CBZ (Table 4), an epoxide ring was formed. Additionally, none of the other signals in either the NMR spectra or the IR spectra were eliminated; so, the rest of the molecule was unchanged.

The fluorescence of the product on the TLC plates (Figure 7) also indicated the probability of the formation of the epoxide. With the addition of a three membered ring on the alkene of CBZ the rotational and vibrational ability of the molecule is greatly reduced. As a result, it is likely that the molecule would fluoresce to release the energy absorbed by the UV light because it cannot release it through increased vibrations. So, because of the possible increased rigidity of the molecule, it is probable that the epoxide of CBZ was formed.

Additionally, the carbamide group was likely unaffected because of the characteristics shown during the quenching and work up of the reaction. With the addition of the NaOH, the product formed an oily mass in organic solvent which did not separate well from the NaOH wash which indicated that the proton on the nitrogen was likely ionized in the strongly basic environment. The additional charge would have attracted the polar water molecules and created an emulsion with the NaOH solution and the dichloromethane. When the pH was lowered by washing the reaction with water, the ionized proton would bond with the carbamide group and, as a result, the product was unable to hold the polar water in the dichloromethane. As a result, the emulsion broke and the two solutions separated. So, the carbamide on the CBZ product was intact, and carbamazepine-10,11-epoxide was formed (Figure 8).

~ *HPLC Calibration Curves for Carbamazepine and Carbamazepine-10,11-epoxide* ~

Method:

All solvents used were HPLC grade. CBZ (25.0mg, 0.106 mmol) was dissolved in 25mL methanol. A volume of 1.25mL of this solution was then diluted into 25mL with methanol. This solution (5mL) was then diluted to 10mL using water so that a 25 μ g/mL (0.106mM) solution of CBZ in a 50:50 solution of methanol:water.

The synthesized CBZ-E (17.8 mg) was dissolved in 25mL of methanol. The resulting solution (1.25mL) was then diluted into 25mL with methanol, and 5mL of this solution was diluted into 10mL with water so that the resulting solution was 17 μ g/mL in 50:50 methanol:water.

The UV spectra for both samples were taken and the optimal absorbance wavelength for each was determined. The HPLC-UV detector was then set to measure the absorbance at these wavelengths (220 nm and 285 nm). The column used was a 5 μ m C18(2) 100 \AA 3.0x150mm (Waters XSelect HSS T3), column temperature was 30°C, run time was 10 min, flow rate was 0.5 mL/min, and the solvent mixture was 47:53 water:methanol. Each sample was injected in the following volumes: 1 μ L, 5 μ L, 10 μ L, 20 μ L, 30 μ L, 40 μ L, and 50 μ L.

The calibration curve calculated for the CBZ was used to determine the purity of the synthesized CBZ-E to enable an accurate calibration curve for CBZ-E to be calculated.

Results:

Figure 13 contains the UV spectra for both CBZ and CBZ-E. The optimal wavelength for CBZ was 220 nm and 285 nm, and the optimal wavelength for CBZ-E was 220 nm. These were the wavelengths used in the HPLC analysis.

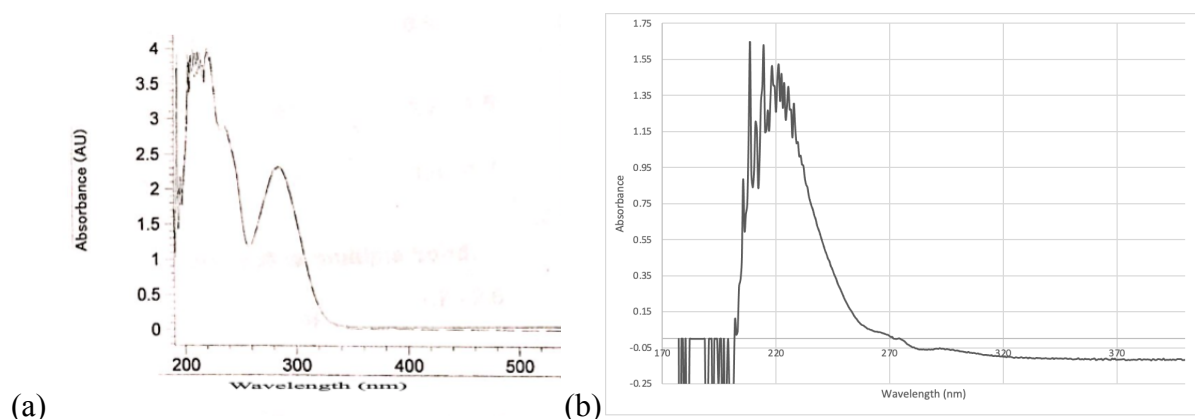


Figure 13. UV spectra for (a) CBZ and (b) CBZ-E.

Figure 14 contains the calibration curves for CBZ at 220 nm and 285 nm. The CBZ eluted from the column at 7.0 min. At 220 nm, the slope of the calibration was $2.87(10^9)\mu\text{mol}^{-1}$, the intercept was $-6.76(10^4)$, and the R^2 value was 1. At 285 nm, the slope of the calibration was $1.24(10^9)\mu\text{mol}^{-1}$, the intercept was $1.24(10^4)$, and the R^2 value was 0.9997. The calibration curve made from the data obtained from the 220 nm absorbance had a higher R^2 value and so this curve was used for the rest of the analysis.

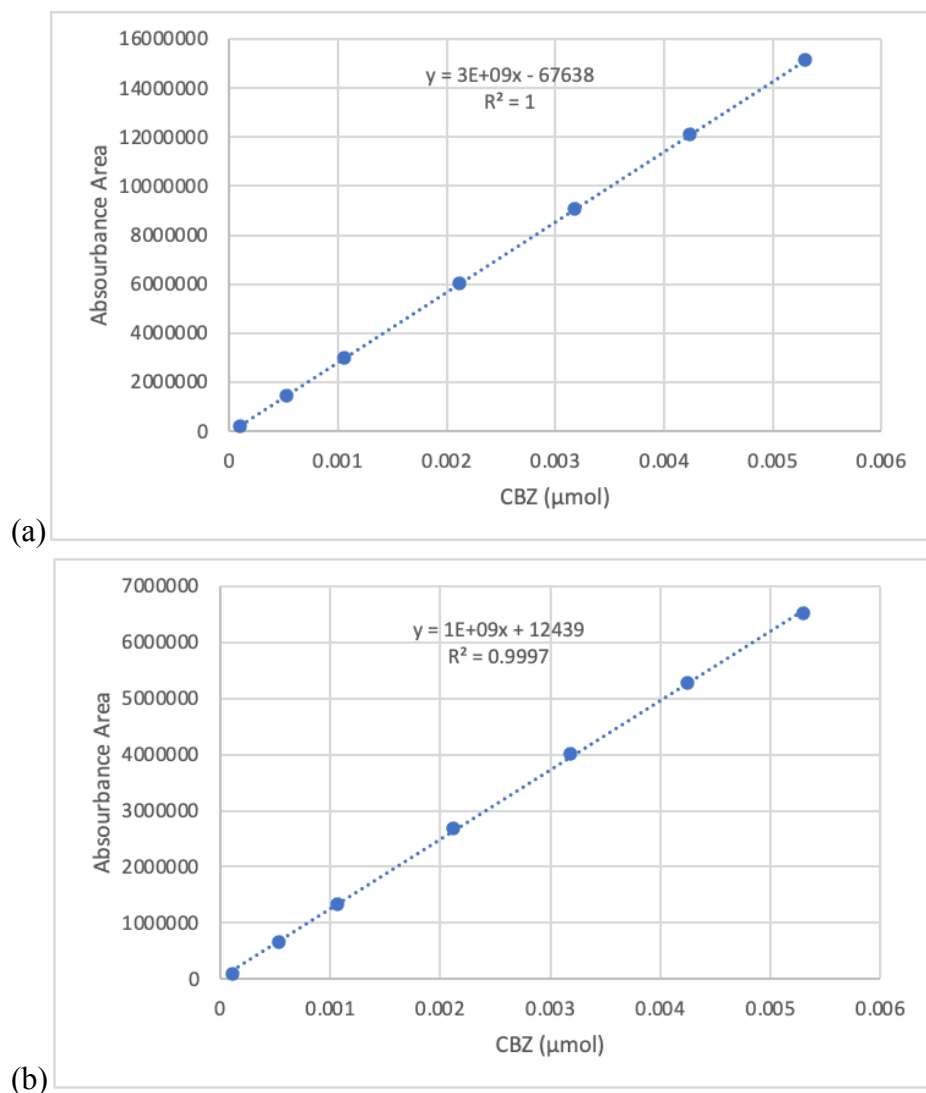


Figure 14. Calibration curve for CBZ at (a) 220 nm and (b) 285 nm.

The CBZ-E eluted at 3.7 min. However, in the HPLC analysis of the synthesized CBZ-E, a peak at 7.0 min was also present indicating the presence of unreacted CBZ (Figure 15). As a result, the actual concentration of CBZ-E was calculated by subtracting the concentration of this peak from the total concentration of the analyzed solution.

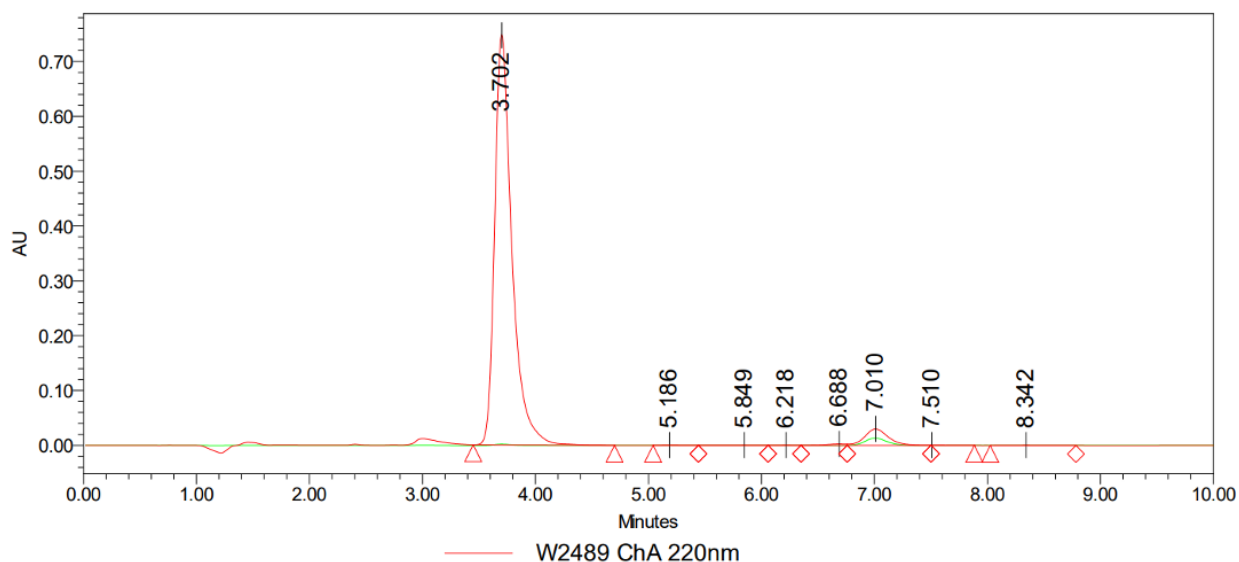


Figure 15. Sample chromatogram of the HPLC analysis of the synthesized CBZ-E indicating unreacted CBZ at 7.010 min.

Figure 16 contains the absorbance of CBZ in the synthesized epoxide solution. Only the last three data points were used to determine the concentration of CBZ in the epoxide solution because these were within the range of the calibration curve. The three calculated concentrations were $0.897\mu\text{g/mL}$, $0.856\mu\text{g/mL}$, and $0.830\mu\text{g/mL}$. These three values were averaged so that the concentration of CBZ in the epoxide solution was $0.861\mu\text{g/mL}$. As a result, the actual concentration of CBZ-E in the epoxide solution was $16.9\mu\text{g/mL}$ rather than $17.8\mu\text{g/mL}$. The percent purity of the synthesized CBZ-E was 95.2%. The total percent yield of the overall synthesis reaction was 76%.

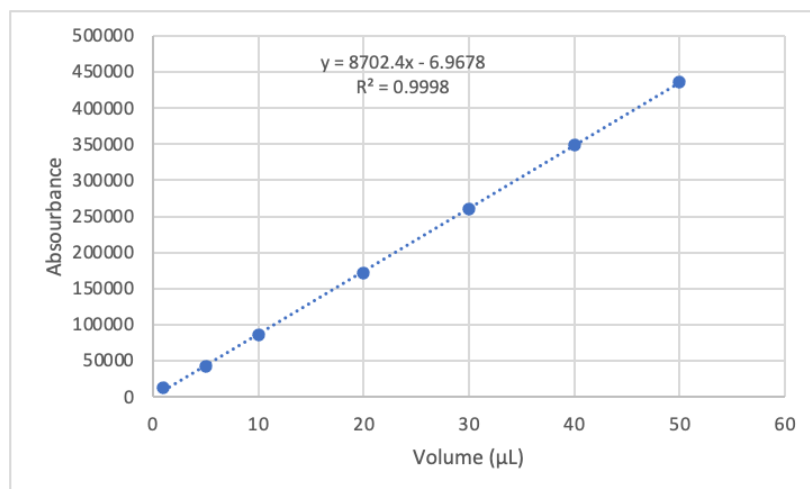


Figure 16. Concentration of unreacted CBZ in the synthesized CBZ-E. Absorbance of CBZ vs the injection volume.

Figure 17 contains the calibration curve for CBZ-E measured at 220 nm. The slope of this line was $2.37(10^9)\mu\text{mol}^{-1}$, the intercept was -15500, and the R^2 value was 1.

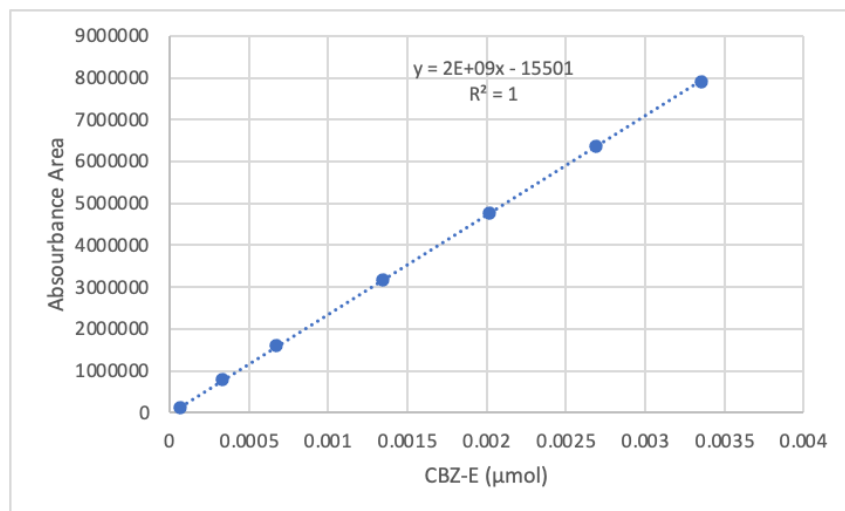


Figure 17. Calibration curve for the absorbance vs amount of CBZ-E (μmol).

Discussion:

The calibration curves were organized so that the amount of analyte passing through the column would be calculated rather than the concentration of the analyte. As a result, when an unknown is compared to these curves, the amount of analyte detected may be divided by the injected volume to determine the concentration of the unknown. This method was used to determine the amount of unreacted CBZ remaining in the synthesized CBZ-E.

Both the CBZ and the CBZ-E had a greater extinction coefficient at 220 nm. Accordingly, the data collected at 220 nm was used to complete the analysis. The peaks at 7.0 min in the synthesized analyte corresponded to the unreacted CBZ, and the amount of CBZ in these peaks was calculated using the CBZ calibration curve. Only the last three peaks were within the range of CBZ concentrations used to make the calibration curve, so only these three peaks were used to determine the CBZ concentration. These values were averaged to determine the concentration of CBZ in the CBZ-E standard (Table 5).

Table 5. Concentration of unreacted CBZ in the CBZ-E standard solution.

Injection Volume (μL)	CBZ (μmol)	Original Concentration ($\mu\text{g/mL}$)
30	0.000114	0.897
40	0.000145	0.856
50	0.000176	0.830
Average	~	0.861

The concentration of CBZ in the standard ($0.861\mu\text{g/mL}$) was then subtracted from the total concentration of analyte in the standard ($17.8\mu\text{g/mL}$) to find a concentration of $16.9\mu\text{g/mL}$

CBZ-E. This concentration was then used to determine the amount of CBZ-E in each injection volume and the calibration curve.

Sample Calculation:

For an injection volume of 40 μ L of the CBZ-E standard an absorbance peak area of 348603 was detected corresponding to the unreacted CBZ. There were 0.000145 μ mol CBZ in the 40 μ L injection, and the concentration of CBZ in the solution was 0.856 μ g/mL.

$$Absorbance = CBZ \times 2.87(10^9)\mu mol^{-1} - 6.76(10^4)$$

$$348603 = CBZ \times 2.87(10^9)\mu mol^{-1} - 6.76(10^4)$$

$$CBZ = 0.000145 \mu mol$$

$$\frac{CBZ}{volume} = \frac{0.000145 \mu mol}{40 \mu L} = 3.624 \times 10^{-6} M$$

$$CBZ \text{ mass conc.} = (3.624 \times 10^{-6} M)(236.269 \text{ g/mol})(\frac{10^6 \mu g}{1 g})(\frac{1 L}{1000 mL}) = 0.856 \mu g/mL$$

This mass concentration was then averaged with the concentrations calculated from the 30 μ L and 50 μ L injections (table 1), and the average was then subtracted from the mass concentration of the standard solution to determine the concentration of CBZ-E in the standard solution. The concentration of CBZ-E was 16.9 μ g/mL, 0.0671 mM.

$$Total \text{ conc.} - CBZ \text{ conc.} = CBZE \text{ conc.}$$

$$17.8 \mu g/mL - 0.856 \mu g/mL = 16.9 \mu g/mL$$

$$(16.9 \mu g/mL) \div (252.27 \text{ g/mol}) = 0.0671 \text{ mM}$$

~ *Solution and Microsome Preparation* ~

The method laid out by Knights *et al* was used as a guide for the metabolism parameters,¹² and the following solutions were made in preparation to perform the metabolism. There were three solutions which had to be prepared for this purpose: 0.1M pH 7.4 potassium phosphate buffer, 10mM NADPH in buffer, and 7.28mM CBZ in methanol.

For the 0.1M pH 7.4 potassium phosphate buffer, 12.147g potassium phosphate dibasic and 4.136g potassium phosphate monobasic were dissolved in 1L deionized water. The resulting pH of the solution was 7.26, so, while the solution was stirred, 1M KOH was added till the pH was 7.40. The solution was parafilmmed and left at room temperature until it was used.

To make the 10mM NADPH solution, 0.248g of NADPH were dissolved in 3mL of the above prepared buffer solution. The NADPH solution was then split into 1.5mL portions and frozen in a -80°C freezer to prevent the decomposition of the NADPH before its use.

To make the 7.28mM CBZ solution, 0.0172g CBZ was dissolved into 10mL of methanol. The volumetric flask was capped, parafilmmed, and placed in the refrigerator to prevent the evaporation of the methanol before the solution was used.

The microsomes (GENTEST[®], Microcosm HuLiver 20+ Donor Mix, 20 mg protein/mL, lot: 1151001) were split into 4 125µL portions and frozen back in the -80°C freezer until they were ready to be used. This would ensure the microsomes would go through as few freeze-thaw cycles as possible which would decrease the chance of the enzymes denaturing or being damaged before their use. This precaution would decrease the potential variation between microsomal metabolisms. However, in the future, the microsomes should be split into volumes divisible by 78µL as this is the volume used in one metabolism trial. Additionally, the number of 78µL

portions in the vial ought to be indicated and updated as the vial on the vial as it is used so that the number of trials left in the vial is easily determined, and the potential for wasted or damaged microsomes is reduced.

~ Microsomal Metabolism of CBZ ~

A preliminary trial metabolism was run to test concentration ranges and the techniques of the method. Originally, the concentration of CBZ in the total assay before quenching was 50 μ M for an enzyme concentration of 0.52 mg protein/mL. However, this concentration of CBZ overwhelmed the system, so the final metabolism concentration of CBZ was reduced to 4.9 μ M. Additionally, in order to guarantee that the system would not run out of energy, the final concentration of NADPH before quenching was increased from 1.0 mM to 1.1 mM. Lastly, each trial was run at 6x the literature volume¹² so that 6 data points could be collected from each assay.

~First Metabolism of CBZ:

Method:

A heating block was set to keep the contents of test tubes at a constant temperature of 37°C. Six assays of the metabolism were run in one test tube. Table 6 contains the volumes for the components of the metabolism trial. The buffer (0.1M pH 7.4 potassium phosphate buffer), NADPH (10 mM NADPH in buffer), and CBZ (7.28 mM CBZ in methanol) solutions were prepared above. The buffer, NADPH, and CBZ were added to the test tube which was then corked and the contents were allowed to incubate in the heating block for 5 min. After 5 min,

the microsomes (20 mg protein/mL) were added, the assay was vortexed, recorked, and the timer was started.

Table 6. Volumes of the reagents in the second metabolism trial.

	Volumes
<i>Buffer</i>	2592 μ L
<i>NADPH</i>	328 μ L
<i>CBZ</i>	2 μ L
<i>Microsomes</i>	78 μ L

Samples were taken from the trial and analyzed at the 0, 10, 20, 40, 60, and 90 min marks. To quench these samples, six 250 μ L volumes of acetonitrile were pipetted into 6 microcentrifuge tubes, and these tubes were placed on ice. At the proper time, 500 μ L of the metabolism trial were pipetted into the corresponding microcentrifuge tube containing the iced acetonitrile. The tube was vortexed and kept on ice until all the time samples had been collected and quenched.

The collected time samples were then centrifuged at 4°C for 5 min with a force of 10000xg. The supernatant was then collected, filtered (0.45 μ m syringe filter), and run through HPLC analysis. If the HPLC analysis was delayed and performed on another day, the samples were frozen at -20°C until the day of the analysis, at which point, the samples were removed from the freezer and thawed. The analysis would then resume as normal.

The HPLC analysis was run using a reverse phase HPLC column at 30°C, with a flow rate of 0.5 mL/min, the UV wavelength was set to 220 nm, the injection volume was 10 μ L, and the solvent mixture was 47:53::water:methanol. Each sample was allowed to run for 10 min

before the next sample was injected. The calibration curve for the CBZ and CBZ-E analysis above was used to determine the concentration of both CBZ and CBZ-E (see previous, pp. 24-29).

Results:

Figure 18 contains the number of μmol of CBZ, CBZ-E, and the combined number of μmol for the two of them in each HPLC injection versus the time of collection. The amount of CBZ remained relatively constant at 0.05 nmol while the amount of CBZ-E grew to a maximum of 0.000024 μmol and began to decrease after its maximum point. Consequently, the total amount of detected CBZ and CBZ-E varied between measurements and followed the trend of the CBZ-E.

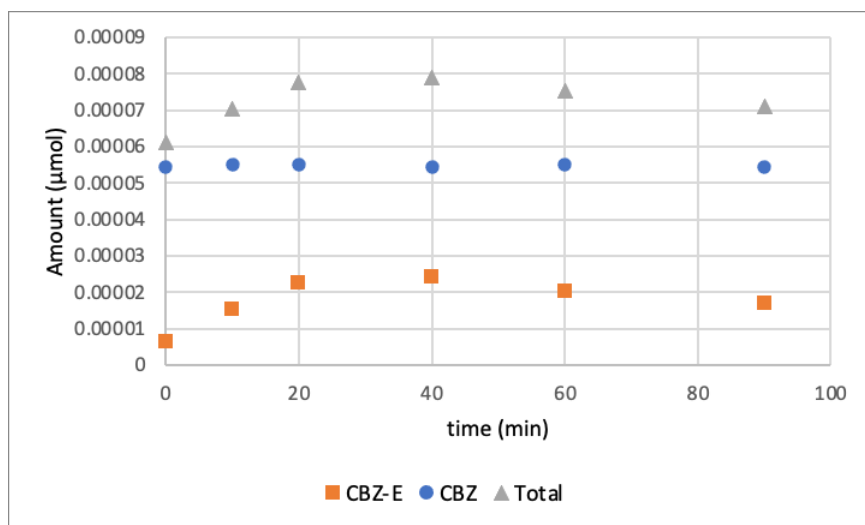


Figure 18. Amount of CBZ (blue), CBZ-E (orange), and the combined (gray) amounts in each HPLC injection.

Discussion:

The decline in the amount of CBZ-E followed by its growth could have been the result of the metabolite CBZ-E being further metabolized, or the epoxide ring could have broken open after being formed. As the epoxide grew in, however, the amount of CBZ did not decrease. This could have been an issue with the precision of the method. To verify these results, a second trial of CBZ metabolism was run with controls.

~Second Metabolism of CBZ with Controls:Method:

The method from the first CBZ metabolism was followed with a few adjustments. Table 7 contains the volumes of the reagents in each assay. Each control contained all the reagents with the exception of one. The volume of the missing reagent was replaced with buffer. Additionally, the time of incubation was adjusted to 0, 10, 20, 30, 40, and 60 min. The samples were incubated, quenched, and analyzed using the method detailed in the first metabolism of CBZ.

Table 7. Volumes for the second metabolism with controls

	Without Microsomes	Without NADPH	Without CBZ	Full Run
<i>Buffer</i>	2670 μL	2920 μL	2594 μL	2592 μL
<i>NADPH</i>	328 μL	~	328 μL	328 μL
<i>CBZ</i>	2 μL	2 μL	~	2 μL
<i>Microsomes</i>	~	78 μL	78 μL	78 μL

Results:

There was no peak for CBZ or the epoxide in the trial without CBZ. Figure 19 contains the amount of CBZ (a) and CBZ-E (b) in each HPLC injection. Some of the sample incubated to 40 min without NADPH was lost so the HPLC vial was not full to the top. As a result, the needle collecting the sample for the injection may not have drawn the correct volume, and the amount of CBZ would have been altered resulting in the unusually low measurement of CBZ in this sample during the analysis.

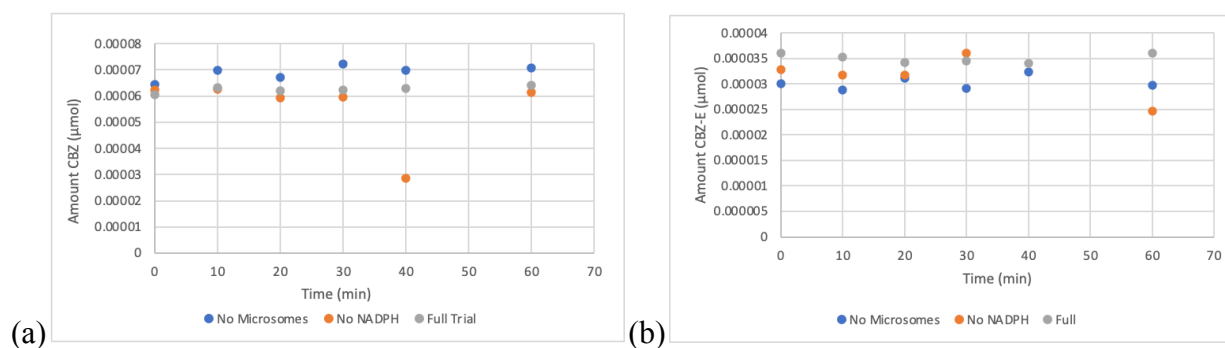


Figure 19. Amount of CBZ (a) and CBZ-E (b) in each HPLC injection vs. the time of incubation.

Both the amount of CBZ and the amount of CBZ-E remained relatively constant at around 0.065 and 0.035 nmol respectively throughout the full incubation (Figure 19). However, the precision of the measurement varied. Additionally, the peak associated with the epoxide was on the edge of the biomass elution at 3.5 min (Figure 20). Thus, it is questionable whether this peak truly and reliably belonged to the epoxide.

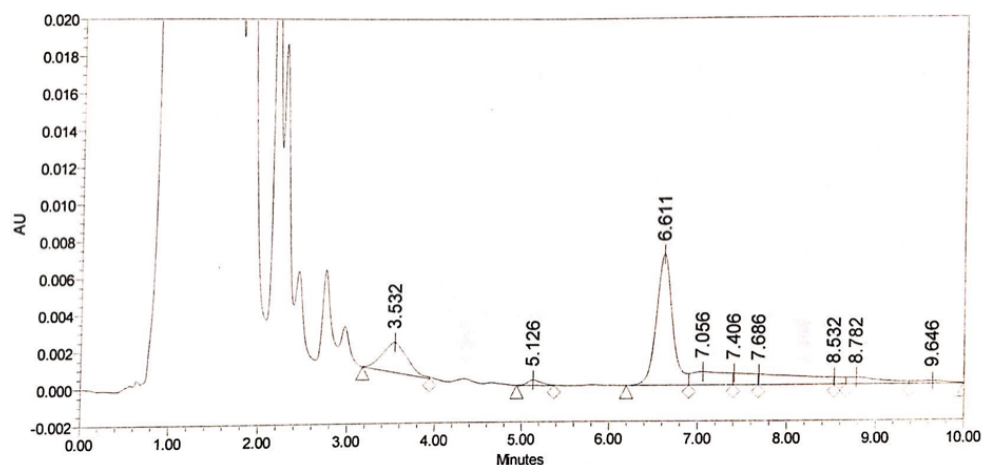


Figure 20. Chromatogram of a representative metabolism sample. CBZ eluted at 6.6 min, and CBZ-E eluted at 3.5 min.

Figure 21 contains the CBZ concentrations from all the trials. The dotted line represents the expected concentration of CBZ ($4.85 \times 10^{-5} \mu\text{mol}/10\mu\text{L}$) if no metabolism occurred. All of the measured concentrations of CBZ were above the expected value.

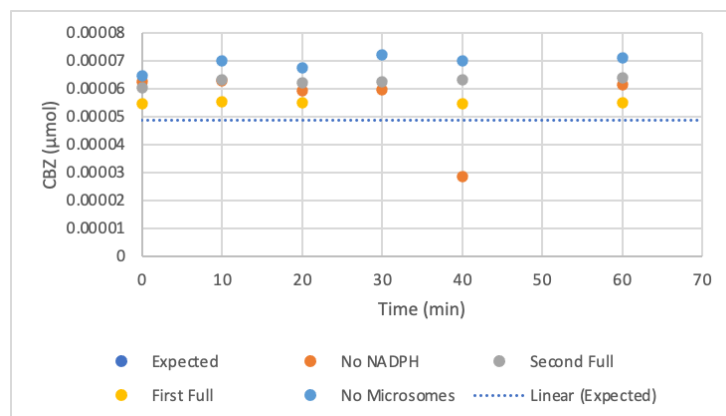


Figure 21. CBZ content in all the trials and a linear representation of what was expected.

Discussion:

Unexpectedly, the epoxide was present from time zero throughout the incubation (Figure 19). Additionally, it did not show the same trend as was seen in the first metabolism of CBZ where the epoxide amount increased and then disappeared (Figure 18). So, it is questionable whether the identified peak belonged to the epoxide in these samples.

Additionally, the CBZ peaks alone were all above the expected peak size (Figure 21). On average, the concentration of CBZ ($6.1 \times 10^{-5} \mu\text{mol}/10\mu\text{L}$) was 1.25 of the actual CBZ concentration ($4.85 \times 10^{-5} \mu\text{mol}/10\mu\text{L}$). If the epoxide peaks were added to these values to calculate the concentration of CBZ before metabolism, the average concentration before metabolism would be $9.1 \times 10^{-5} \mu\text{mol}/10\mu\text{L}$. This value is 1.91 of the actual concentration of CBZ ($4.85 \times 10^{-5} \mu\text{mol}/10\mu\text{L}$). So, it is likely that the peak associated with the epoxide did not belong to the epoxide.

One potential cause of the increase in the CBZ concentration was during the process of filtration, some of the solvent may have been left in the filter while the solute passed through, causing the concentration of the filtrate to be greater. Another potential cause was during the process of centrifugation, the removal of the microsomal proteins reduced the volume of the sample. However, the volume removed was primarily microsomes, and as a result, the concentration of all the other solutes were increased.

Conclusion

We have successfully synthesized and characterized the epoxide of CBZ using traditional organic synthesis. To our knowledge, this is the first report of the chemical synthesis of this compound. Further, we have measured the extinction coefficient of both species toward the end of quantifying these compounds in metabolic incubations. HPLC conditions have been developed to separate CBZ and CBZ-E from each other and from the microsomal sample matrix.

Unexpectedly, the human microsomal metabolism of CBZ has given irreproducible results, with only one trial potentially showing the expected epoxide metabolite. The reason for the lack of metabolic activity is unknown at this time. Going forward, the UV-vis spectra of NADPH and the phosphate buffer should be acquired, and their time of elution should be determined. Whether these compounds appear in the 220 nm detection range, and where they elute may influence the data collected for CBZ and CBZ-E. The method would then be adjusted accordingly. Additionally, the elution time of the biomaterial from the microsomes was too close to the expected elution time of the epoxide (Figure 20). To resolve this issue, the methanol concentration in the mobile phase should be increased so that the epoxide would elute at a later time, giving the biomaterial more time to clear the column so as not to interfere with the epoxide detection. By drawing out the times of elution, the epoxide would elute at a later time and clear the biomass signal. Also, if the CBZ-E is metabolized further, the signal from these metabolites, as they would elute earlier than the CBZ-E, may potentially clear the biomass as well. As a result, the appearance of these metabolites over the course of the incubation would be able to be detected and monitored.

To investigate the problem of the lack of metabolism, a few courses of action may be pursued. In the work done by Kerr *et al*, the microsomal protein concentration was 1 mg/mL.¹⁰ However, in this investigation, a microsomal protein concentration of 0.52 mg/mL was used. In future investigations, the microsomal content ought to be doubled to determine whether the low concentration of microsomal protein prevented drug metabolism.

Our efforts will continue to examine this metabolic pathway as we look toward using it to probe drug-drug interactions.

References

1. Pharmaceutical Research and Manufacturers of America. *The Process Behind New Medicines*. Biopharmaceutical Research & Development, **2015**.
http://phrma-docs.phrma.org/sites/default/files/pdf/rd_brochure_022307.pdf (accessed 2021-11-15).
2. Heinemann, F. S.; Ozols, J. Isolation and Structural Analysis of Microsomal Membrane Proteins. *Front Biosci* **1998**, 3, d483-493. DOI: 10.2741/a295.
3. Hoehn, K.; Marieb, E. *Human Anatomy and Physiology*; Pearson Education Inc, **2019**.
4. Anzenbacher, P.; Zanger, U. M. *Metabolism of Drugs and Other Xenobiotics*; John Wiley & Sons, Incorporated: Weinheim, GERMANY, **2012**. Chapter 1.1
5. Gad, S. C.; Gad, S. C. *Preclinical Development Handbook: ADME and Biopharmaceutical Properties*; John Wiley & Sons, Incorporated: Hoboken, UNITED STATES, **2008**. Chapter 18
6. Zuber, R.; Anzenbacherová, E.; Anzenbacher, P. Cytochromes P450 and Experimental Models of Drug Metabolism. *Journal of Cellular and Molecular Medicine* **2002**, 6 (2), 189–198. DOI: 10.1111/j.1582-4934.2002.tb00186.x.
7. Martignoni, M.; Groothuis, G. M. M.; de Kanter, R. Species Differences between Mouse, Rat, Dog, Monkey and Human CYP-Mediated Drug Metabolism, Inhibition and Induction. *Expert Opinion on Drug Metabolism & Toxicology* **2006**, 2 (6), 875–894. DOI: 10.1517/17425255.2.6.875.

8. Krest, C. M.; Onderko, E. L.; Yosca, T. H.; Calixto, J. C.; Karp, R. F.; Livada, J.; Rittle, J.; Green, M. T. Reactive Intermediates in Cytochrome P450 Catalysis. *J Biol Chem* **2013**, 288 (24), 17074–17081. DOI: 10.1074/jbc.R113.473108.
9. Basheer, L.; Kerem, Z. Interactions between CYP3A4 and Dietary Polyphenols. *Oxid Med Cell Longev* **2015**, 2015, 854015. DOI: 10.1155/2015/854015.
10. Kerr, B. M.; Thummel, K. E.; Wurden, C. J.; Klein, S. M.; Kroetz, D. L.; Gonzalez, F. J.; Levy, R. H. Human Liver Carbamazepine Metabolism. Role of CYP3A4 and CYP2C8 in 10,11-Epoxy Formation. *Biochem Pharmacol* **1994**, 47 (11), 1969–1979. DOI: 10.1016/0006-2952(94)90071-x.
11. STYRENE OXIDE. *Org. Synth.* **1928**, 8, 102. DOI: 10.15227/orgsyn.008.0102.
12. Knights, K. M.; Stresser, D. M.; Miners, J. O.; Crespi, C. L. In Vitro Drug Metabolism Using Liver Microsomes. *Current Protocols in Pharmacology* **2016**, 74 (1). DOI: 10.1002/cpph.9.